PLOS ONE

Utilizing digital pathology to quantify stromal caveolin-1 expression in malignant and benign ovarian tumors: Associations with clinicopathological parameters and clinical outcomes

Daryoush Saeed-Vafa[1], Douglas C. Marchion[2], Susan M. McCarthy[1¤a], Ardeshir Hakam[1], Alexis Lopez[1], Robert M. Wenham[3], Sachin M. Apte[3¤b], Dung-Tsa Chen[4], Anthony M. Magliocco[1¤c], Johnathan M. Lancaster[3¤d], Brett M. Reid[5‡], Jennifer B. Permuth[5‡]*

1 Department of Anatomic Pathology, H. Lee Moffitt Cancer Center and Research Institute, Tampa, Florida, United States of America, 2 Tissue Core-Biospecimen Processing Laboratory, H. Lee Moffitt Cancer Center and Research Institute, Tampa, Florida, United States of America, 3 Department of Gynecologic Oncology, H. Lee Moffitt Cancer Center and Research Institute, Tampa, Florida, United States of America, 4 Department of Biostatistics and Bioinformatics, H. Lee Moffitt Cancer Center and Research Institute, Tampa, Florida, United States of America, 5 Department of Cancer Epidemiology, H. Lee Moffitt Cancer Center and Research Institute, Tampa, Florida, United States of America

¤a Current address: HistogeneX, Naperville, Indiana, United States of America
¤b Current address: Huntsman Cancer Institute, Salt Lake City, Utah, United States of America
¤c Current address: Protean BioDiagnostics, Orlando, Florida, United States of America
¤d Current address: Regeneron Science to Medicine, Tarrytown, New York, United States of America
‡ BMR and JBP are joint senior authors on this work.
* jenny.permuth@moffitt.org

OPEN ACCESS

Abstract

Loss of stromal caveolin-1 (Cav-1) is a biomarker of a cancer-associated fibroblast (CAF) phenotype and is related to progression, metastasis, and poor outcomes in several cancers. The objective of this study was to evaluate the clinical significance of Cav-1 expression in invasive epithelial ovarian cancer (OvCa). Epithelial and stromal Cav-1 expression were quantified in serous OvCa and benign ovarian tissue in two, independent cohorts–one quantified expression using immunohistochemistry (IHC) and the other using multiplex immunofluorescence (IF) with digital image analysis designed to target CAF-specific expression. Cav-1 expression was significantly downregulated in OvCa stroma compared to non-neoplastic stroma using both the IHC ($p = 0.002$) and IF ($p = 1.8 \times 10^{-13}$) assays. OvCa stroma showed Cav-1 downregulation compared to tumor epithelium with IHC ($p = 1.2 \times 10^{-24}$). Conversely, Cav-1 expression was higher in OvCa stroma compared to tumor epithelium with IF ($p = 0.002$). There was moderate correlation between IHC and IF methods for stromal Cav-1 expression ($r^2 = 0.69$, $p = 0.006$) whereas there was no correlation for epithelial expression ($r^2 = 0.006$, $p = 0.98$). Irrespective of the staining assay, neither response to therapy or overall survival correlated with the expression level of Cav-1 in the stroma or tumor epithelium. Our findings demonstrate a loss of stromal Cav-1 expression in ovarian serous carcinomas.

Studies are needed to replicate these findings and explore therapeutic implications, particularly for immunotherapy response.

Introduction

Ovarian carcinoma (OvCa) is the fifth leading cause of cancer-related deaths among women in the United States. In 2020, an estimated 21,750 new cases of OvCa and 13,940 related deaths occurred, making it the most deadly of all gynecologic cancers [1]. Due to non-specific symptoms and lack of early detection methods, nearly 80% of women present with advanced stage (III/IV) disease with a 5-year relative survival rate of approximately 30% [1]. Despite standard treatment, which includes surgical debulking followed by platinum-based chemotherapy, most women succumb to persistent or recurrent platinum-resistant disease. Thus, there is a dire need to discover novel biomarkers for OvCa that are associated with clinical outcomes and could potentially serve as therapeutic targets.

The tumor microenvironment is a critical component of ovarian carcinogenesis and immune response that can yield information relevant to prognosis and chemoresistance [2–7]. Cancer-associated fibroblasts (CAFs) are the most abundant cells in the tumor microenvironment and are known to promote tumor growth, invasion, and metastasis [8–12] and impact the efficacy of chemotherapy [8, 10–13]. Ovarian CAFs are genetically more stable than tumor cells [14], making them less prone to developing chemoresistance and therefore excellent therapeutic targets. However, the clinical significance of proteins associated with CAFs in OvCa is largely unexplored.

Caveolin-1 (Cav-1) belongs to a family of scaffolding proteins that regulate signal transduction and cell proliferation [15] and has emerged as a marker of a lethal CAF phenotype. Specifically, the absence or loss of stromal Cav-1 expression has been shown to activate epithelial AKT signaling [13, 16] and be a powerful predictor of poor outcomes in numerous malignancies, including breast, prostate, pancreatic, papillary thyroid cancers, and melanoma [8–15, 17–20]. Furthermore, the reduced expression of Cav-1 in the 'reactive' or desmoplastic stroma of malignant tumors correlates with more aggressive disease and advanced stage [12–14]. Investigations in OvCa have found Cav-1 functions as a tumor suppressor gene and is significantly downregulated in ovarian cancer cell lines and carcinomas which promotes tumor growth, survival, invasion, and metastasis [21–25]. Additionally, stromal Cav-1 expression has been detected in benign ovarian serous tumors but is largely absent in malignant and borderline ovarian serous tumors [26]. Several studies have observed loss of Cav-1 staining specifically in OvCa stromal cells, suggesting Cav-1 may be a marker of CAFs and poor survival in OvCa, as in other cancers. Supporting this role, reduced Cav-1 mRNA expression has been associated with poor survival in serous carcinomas from The Cancer Genome Atlas. Further, stromal Cav-1 expression has been correlated with more aggressive ovarian serous tumors [6, 26]. However, a recent study evaluating Cav-1 expression in OvCa stroma did not detect an association with survival [26] but this may be due to the small sample size (n = 31) or quantification of expression as absent or present. Thus, it is unclear whether stromal Cav-1 expression could serve as a prognostic and therapeutic marker for OvCa.

The purpose of this study was to comprehensively quantify stroma and epithelium Cav-1 expression and to explore the relationship with clinicopathologic variables, response to first-line platinum-based chemotherapy, and survival. We evaluated tissue microarrays (TMAs) comprised of human serous carcinomas and benign ovarian tissue from two independent,

relatively large cohorts of women diagnosed and treated at our National Cancer Institute-designated Comprehensive Cancer Center. We evaluated one cohort using an immunohistochemistry (IHC) assay and semi-quantitative scoring and the other with a multiplex immunofluorescence (IF) assay quantified using automated digital image analysis because of its more precise and objective quantification of protein expression [27].

Materials and methods

Study populations and clinical data

The study population included two cohorts diagnosed and treated at Moffitt Cancer Center, with the entire project conducted in accordance with full institutional review board approval after obtaining written informed consent. This study has been carried out in accordance with the ethical principles for medical research involving human subjects, set by the Declaration of Helsinki and was approved by the University of South Florida Institutional Review Board (IRB#: Pro00008518). Each cohort included subjects with malignant and benign disease. Malignant cases were defined as women with primary pathologically-confirmed invasive epithelial OvCa treated with surgery followed by platinum-based therapy. Benign cases included women who underwent surgery for benign gynecologic conditions. Both groups of women donated tissue specimens under the auspices of an institutional tissue banking protocol. The first cohort (Cohort 1) comprised subjects who underwent surgery between 1987 and 2010, whereas the second cohort (Cohort 2) underwent surgery between 2000 and 2012. Since OvCa incidence and mortality is highest in non-hispanic whites[1] and most OvCas are of the serous subtype, which is etiologically distinct from other histologies [28], our analyses focused on invasive serous adenocarcinomas among non-Hispanic whites.

Demographic and clinical data was obtained from the Moffitt Cancer Registry (age at diagnosis, histology, pathologic grade and stage, CA-125 levels, debulking status, treatment regimens and response, recurrence) supplemented by the medical record, and the National Death Index (for vital status). For purposes of this study, overall survival was defined as the time between the date of diagnosis and the date of death or last contact. Treatment response was retrospectively determined using standard criteria for patients with measurable disease using World Health Organization guidelines [28]. CA-125 was used to classify response in the absence of a measurable lesion [29, 30]. Complete clinical responders (CR) had complete disappearance of all measurable disease for 4 weeks after completing first-line platinum-based chemotherapy, or in the absence of measurable lesions, a normalization of the CA-125 level for at least 4 weeks after therapy and were therefore initially chemosensitive. Patients who demonstrated a partial response (defined as a 50% or greater reduction in tumor burden obtained from measurement of each bi-dimensional lesion for at least 4 weeks, or a drop in CA-125 by >50% for at least 4 weeks after completing therapy), no response (had stable disease), or progressed during adjuvant therapy were considered chemoresistant and thus classified as incomplete responders (IR).

Tissue microarrays

We utilized two ovarian tissue microarrays (TMAs) in this study. The first was an existing TMA (TMA 1) of Cohort 1 subjects that included 100 OvCa cases selected based on treatment response (50 CRs and 50 IRs) and 35 benign cases. The second (TMA 2) was constructed specifically for this investigation from Cohort 2 subjects that included 128 unselected OvCa cases and 30 benign cases. TMA 2 included a subset of OvCa cases (n = 11) sampled in TMA 1/ Cohort 1. Cores for both TMAs were obtained from formalin-fixed paraffin-embedded tissue blocks that had been stored at room temperature. Hematoxylin-and-eosin (H&E) stained

slides from selected blocks were reviewed by a pathologist with expertise in gynecologic tumors (AH, AL) to confirm the diagnosis, in accordance with the 2018 WHO guidelines, and select regions of interest (ROI). For the established TMA 1, OvCa sampling included single cores punched from macrodissected tumor tissue. Benign case samples included single cores from normal ovarian tissue. For TMA 2, four ROIs were preferentially sampled for OvCa cases: 1) abundant CAF-enriched tumor stromal cells immediately adjacent to the tumor epithelium; 2) areas of abundant tumor epithelial cells; 3) paired adjacent normal ovarian and/or fallopian epithelial tissue; 4) normal non-neoplastic stroma with a high abundance of normal fibroblasts that are morphologically distinct from CAFs [8, 9]. For each ROI on TMA 2, duplicate 1.0 mm cores were sampled to account for tissue heterogeneity and the cores were placed side-by-side on a recipient microarray block. Samples for benign cases in TMA 2 included multiple cores from normal stroma and/or epithelium tissues, when present. The Moffitt Tissue Core Facility constructed the TMAs using a precision instrument (Tissue Arrayer, Beecher Instruments, WI) per standard protocols.

Immunohistochemistry and scoring, TMA 1/Cohort 1

A rabbit polyclonal anti-Cav-1 IgG antibody (Santa Cruz Biotechnology, Santa Cruz, CA) was used for immunohistochemical (IHC) staining of 3 micron thick sections of the TMA block as previously described [31]. A board-certified pathologist (AH) scored the stains semi-quantitatively by multiplying the mean signal intensity scores by the percentage of positive cells. ROIs were identified and scores were calculated separately for each ROI. Tumor samples were scored for tumor epithelium and adjacent stroma. Benign samples were scored for normal stroma and epithelium regions. Staining intensity was scored as follows: 0 (negative; no staining), 1 (weak), 2 (moderate), and 3 (strong). The percentage of positive cells was scored as: 0 (0%), 1 (1–33%), 2 (34–66%), and 3 (67–100%).

Immunofluorescence and digital image analysis, TMA 2/Cohort 2

A rabbit polyclonal anti-Cav-1 IgG antibody (Santa Cruz lot: G0314) was used for immunofluorescent (IF) staining of TMA 2 via a standard multiplexing protocol (S1 File). The AQUA® system was used to perform digital image analysis (DIA) on the stained virtual slides generated by the Aperio ScanScope®FL fluorescent scanner. We designed an algorithm to target and quantify Cav-1 expression within the fibroblasts (i.e. the stroma compartment) and the tumor epithelial cells (i.e. the tumor epithelial compartment). The algorithm was designed such that the stroma compartment was defined by the presence of the mesenchymal vimentin signal (fibroblast intermediate filament stain; local to cytoplasm) and the DAPI signal (dsDNA stain; local to nucleus). However, vimentin is a ubiquitous mesenchymal marker that has the potential to stain a variety of cell types including tumor epithelial cells. To ensure that only the fibroblasts were considered in the Cav-1 stroma expression, pixels expressing both vimentin and pancytokeratin (epithelial stain; local to cytoplasm) were excluded from stroma compartment calculations. Ultimately, Cav-1 AQUA® scores (nuclear, cytoplasmic, and complete cell (overall)) were obtained for the stroma compartment, as well as for the tumor epithelial compartment for each TMA core. The AQUA® score was calculated from the sum of the target pixel intensity divided by the compartment area and normalized for image exposure time to make them directly proportional to protein concentration (molecules per unit area) [32]. For purposes of this study, only the overall scores (i.e. the total amount of Cav-1 expressed in the complete cell) within the different compartments (stroma or epithelium) were used for each core. For duplicate cores from the same participant, the mean compartment score was used for statistical analysis.

Statistical analysis

In our analysis, we excluded patients who received neo-adjuvant chemotherapy before surgery or had tissues sampled from recurrent disease. Further, cases diagnosed with histological sub-types other than serous were excluded (Cohort 1 n = 3, Cohort 2 n = 23). Cav-1 expression was compared by the following clinicopathologic features: age (young, ≤65 years, versus old > 65 years), pathologic grade (low-grade versus high-grade), pathologic stage (early-stage I/II versus advanced-stage III/IV), response to therapy (complete responders (CR)/ chemosensitive versus incomplete responders (IR)/ chemoresistant), and survival (long-term survivors of > 60 months versus short-term survivors of ≤ 36 months). For each cohort, the non-parametric Wilcoxon rank-sum test was used to compare the median difference in Cav-1 expression between clinicopathologic subgroups. Logistic regression was used to examine the association of Cav-1 expression with response to chemotherapy including adjustment for significant prognostic factors. The associations between Cav-1 expression and OS were visually assessed using Kaplan-Meier survival curves and log-rank tests. IHC score was dichotomized as the presence (1,2) or absence (0) of Cav-1, consistent with previous studies [31]. IF expression was dichotomized using the median expression as the cutoff. Cox proportional hazards regression was used to estimate the independent association of continuous Cav-1 expression with OS, controlling for significant clinical covariates.

Results

Characteristics of study participants, Cohort 1

A total of 106 subjects were evaluated including 73 serous OvCa cases (Table 1) with chemo-naïve primary tumor tissue sampled and 33 controls with benign ovarian disease. All cases were treated with chemotherapy and 37 (51%) displayed a complete response, reflecting the TMA selection criteria. The average age at diagnosis was 62 (range: 33–83, median = 63) and almost all were diagnosed at an advanced stage (III/IV, n = 72) with high-grade (n = 70) disease that was greater than 50mm in size (n = 64; not assessed for n = 7). Clinical follow-up for overall survival averaged 76.9 months after diagnosis (standard deviation, SD = 91.4, range = 3.6 to 392.9). A total of 65 (89%) of cases died during follow-up with 28 long-term and 36 short-term survivors.

Expression of Cav-1 using immunohistochemistry, Cohort 1

Representative immunohistochemical staining of Cav-1 is shown in Fig 1. For both tumor and benign ovarian tissue, higher expression of Cav-1 was observed in the epithelial regions as compared to stromal regions. Tumor epithelial Cav-1 expression averaged 8-fold higher than adjacent stroma (mean 2.56 vs 0.29, p = 8.7×10^{-19}) while benign ovarian epithelium had 2.5 fold higher expression compared to normal stroma (mean 3.06 vs. 0.88, p = 3.7×10^{-9}). Expression of Cav-1 in benign stroma was two-fold higher than in tumor stroma (p = 0.003). No difference in epithelial expression was observed between benign and tumor tissues (p = 0.63).

Expression of Cav-1 was compared across clinicopathologic characteristics (Table 1). Cases with an incomplete response to therapy had a slightly lower expression of Cav-1 in the stroma as compared to those with a complete response (p = 0.07). Additionally, short term survivors and patients with lymph node involvement (pN) had a slightly lower expression of stromal Cav-1; however, these differences were not statistically significant (p = 0.10 and 0.30, respectively). No difference was observed in the expression of Cav-1 in either the stroma or epithelium by age.

The median overall survival was 40.6 months for OvCa patients. For patients with presence of Cav-1 (Hscore>0) in the epithelium, survival time was comparable to those with an absence

Table 1. Immunohistochemical Cav-1 expression in serous ovarian cancer by clinical characteristics in Cohort 1.

Outcome	N (%)[a]	Tumor Cav-1 Expression, mean (SD)		Mean Δ (SD)
		Stroma	**Epithelium**	
Overall	73	0.29 (0.74)	2.56 (1.53)	-2.22 (1.28)
				p = 8.7x10^{-19}
Age at Diagnosis				
< = 65 years	41 (56%)	0.28 (0.72)	2.59 (1.43)	-2.23 (1.12)
>65 years	32 (44%)	0.31 (0.78)	2.53 (1.67)	-2.22 (1.48)
		p = 0.85	*p = 0.99*	*p = 0.95*
Response to Therapy				
Complete	37 (51%)	0.38 (0.76)	2.57 (1.52)	-2.19 (1.33)
Incomplete	36 (49%)	0.20 (0.72)	2.56 (1.56)	-2.26 (1.24)
		p = 0.07	*p = 0.96*	*p = 0.57*
Nodal Status (pN)[b]				
Not involved	35 (78%)	0.43 (0.98)	2.66 (1.47)	-2.23 (1.17)
Involved	10 (22%)	0.10 (0.32)	2.20 (1.87)	-2.10 (1.66)
		p = 0.30	*p = 0.35*	*p = 0.85*
Survival				
Long-term (>60 months)	28 (44%)	0.37 (0.81)	2.37 (1.71)	-2.00 (1.46)
Short-term (≤36 months)	36 (56%)	0.19 (0.71)	2.57 (1.57)	-2.28 (1.28)
		p = 0.10	*p = 0.78*	*p = 0.36*

SD, standard deviation. P-values comparing expression by clinical subgroups were calculated from Wilcoxon rank sum test. P-values comparing mean difference by clinical subgroups were calculated from Student's t-test.

[a] Survival groups do not include 9 cases with follow-up <36 months or death <60 and >36 months.

[b] pN stage was not assessed for 28 cases that were stage III/IV.

https://doi.org/10.1371/journal.pone.0256615.t001

of Cav-1 (median survival 45.0 vs. 33.5 months, respectively, p = 0.36; Fig 2A). Conversely, patients with presence of stromal Cav-1 expression had longer survival (median 73.3 months) as compared those with an absence of stromal Cav-1 (31.4 months), which was suggestive of an association (p = 0.09, Fig 2B). However, after adjustment for age and response to therapy there was no difference in stromal Cav-1 expression by survival (Hazard Ratio, HR = 0.83, 95% CI = 0.58–1.19, p = 0.31; S1 Table). Survival did not differ by epithelial Cav-1 expression in adjusted analysis (HR = 0.99, 95% CI = 0.84–1.16, p = 0.89; S1 Table).

Characteristics of study participants, Cohort 2

A total of 135 subjects were evaluated including 105 with pathological diagnosis of serous OvCa (Table 2) and 30 controls with benign ovarian tissue. The average age at OvCa diagnosis was 60 years (range: 24–83, median = 62) and the majority presented with advanced (85%), high-grade (95%) disease, similar to our prior cohort. OvCa cases were unselected for response to therapy with most (77%) having a complete response. Additionally, 80 cases were optimally debulked. Patients were followed for an average of 60 months (SD = 44.8, range = 5.2 to 199.0) with 40 short-term and 45 long-term survivors.

Expression of Cav-1 using immunofluorescence, Cohort 2

Cav-1 expression in stroma and epithelium regions was quantified using immunofluorescence staining for both benign ovarian and OvCa tissues (Fig 3). Similar to the IHC analysis, the expression of Cav-1 in benign stroma was significantly higher than in the tumor stroma, with
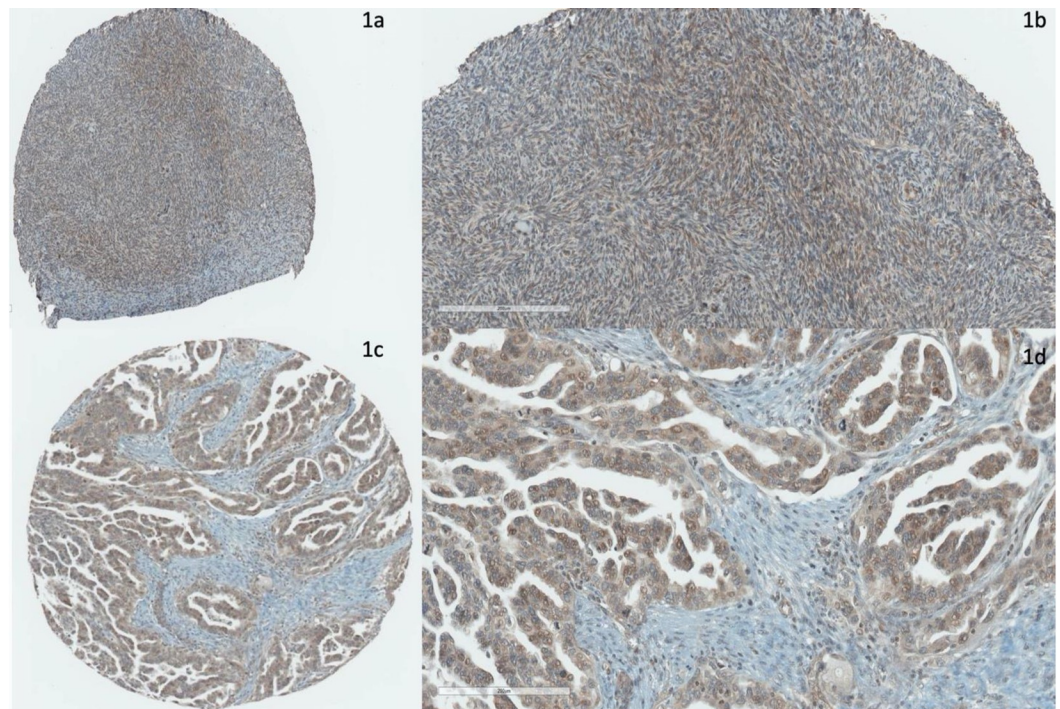
Fig 1. Immunohistochemical expression of Cav-1 in ovarian tissue. (a-b) Normal (benign) ovarian stroma stained with Cav-1 via immunohistochemistry. The fibroblasts in the benign ovarian stroma stain strongly positive for Cav-1. (c-d) High-grade ovarian serous adenocarcinoma stained with Cav-1 via immunohistochemistry. The tumor epithelial cells stain strongly positive for Cav-1, while the fibroblasts in the surrounding desmoplastic stroma stain weakly positive to negative for Cav-1.

https://doi.org/10.1371/journal.pone.0256615.g001
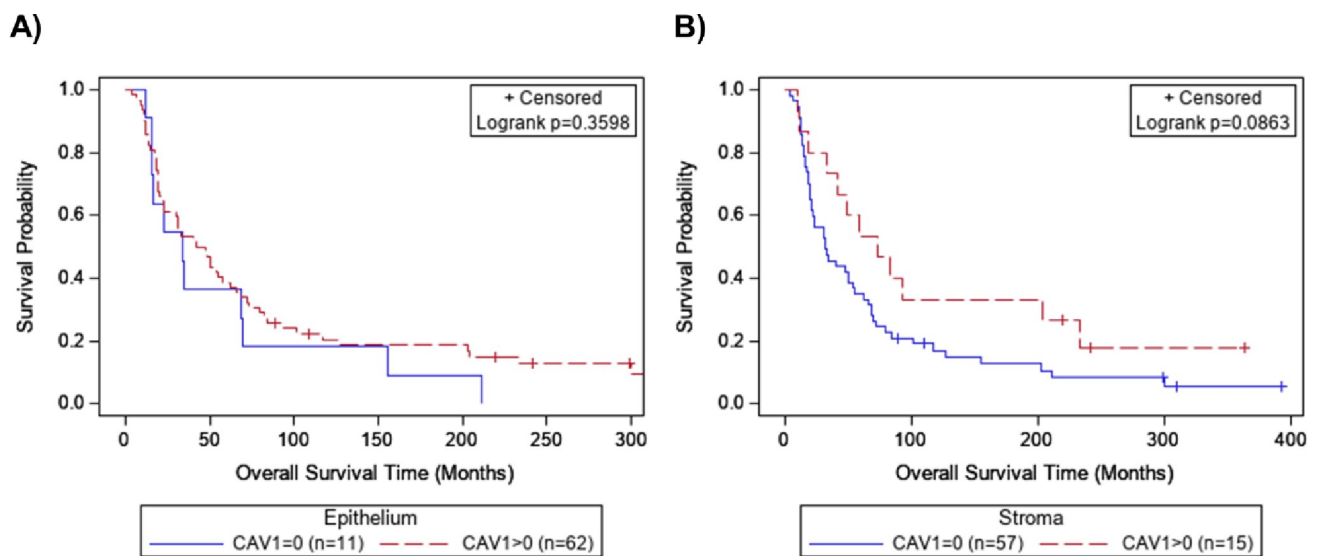
Fig 2. Overall survival of serous ovarian cancer by expression of Cav-1 in Cohort 1. Kaplan-Meier survival curves for Cohort 1 by presence of Cav-1 immunohistochemical expression in the (A) tumor epithelium and (B) stroma using an immunohistochemistry H-score of zero as a cutoff.

https://doi.org/10.1371/journal.pone.0256615.g002

Table 2. Immunofluorescent Cav-1 expression in serous ovarian cancer by clinical characteristics in Cohort 2.

Outcome	N (%)[a]	Tumor Cav-1 Expression, median (SD)		Mean Δ (SD)
		Stroma	Epithelium	
Overall	105	152.6 (43.7)	124.0 (52.4)	15.7 (44.2)
				p = 0.01
Age at Diagnosis				
< = 65 years	60 (57%)	147.2 (43.1)	124.5 (39.08)	14.69 (42.5)
>65 years	45 (43%)	154.6 (41.8)	122.8 (65.01)	17.12 (46.7)
		p = 0.03	*p = 0.23*	*p = 0.78*
Grade				
Low	5 (5%)	169.2 (57.6)	184.2 (106.1)	-30.2 (62.3)
High	100 (95%)	152.4 (43.2)	123.4 (47.5)	18.0 (42.2)
		p = 0.55	*p = 0.14*	*p = 0.16*
Stage				
Early (I/II)	17 (17%)	145.3 (45.3)	122.2 (51.3)	11.8 (47.5)
Advanced (III/IV)	85 (85%)	154.8 (43.4)	122.8 (52.9)	18.2 (43.2)
		p = 0.26	*p = 0.60*	*p = 0.61*
Tumor size (pT)[b]				
>1mm—< = 20mm	10	128.5 (23.2)	104.6 (25.5)	8.5 (39.9)
>20mm—< = 50mm	13	154.8 (50.5)	139.0 (56.1)	7.1 (49.2)
>50mm	78	154.9 (44.6)	122.6 (54.8)	18.9 (44.5)
		p = 0.04	*p = 0.28*	*p = 0.57*
Nodal Status (pN)[c]				
Not involved	42	148.5 (40.5)	122.5 (56.7)	9.4 (45.3)
Involved	14	153.5 (54.9)	139.6 (37.8)	16.6 (41.5)
		p = 0.67	*p = 0.18*	*p = 0.58*
Response to Therapy				
Complete	78 (77%)	150.7 (36.7)	124.5 (52.5)	14.2 (42.3)
Incomplete	23 (23%)	154.4 (58.7)	113.5 (55.6)	18.3 (47.5)
		p = 0.95	*p = 0.73*	*p = 0.71*
Surgical Debulking				
Optimal (NED or <1mm)	80 (79%)	149.9 (43.7)	126.4 (50.9)	12.2 (42.7)
Suboptimal (>1mm)	21 (21%)	154.9 (41.8)	111.8 (32.1)	29.8 (31.8)
		p = 0.68	*p = 0.26*	*p = 0.04*
Survival				
Long-term (>60 months)	45 (53%)	148.9 (39.1)	116.1 (50.0)	9.7 (42.1)
Short-term (≤36 months)	40 (47%)	155.0 (43.7)	123.4 (50.3)	25.3 (37.6)
		p = 0.08	*p = 0.62*	*p = 0.07*

NED, No evidence of disease. P-values comparing expression by clinical subgroups were calculated from Wilcoxon rank sum test (2 groups) or Kruskal-Wallis test (>2 groups). P-values comparing mean difference by clinical subgroups were calculated from Student's t-test (2 groups) or ANOVA (>2 groups).

[a] Some variables do not total to 105 due to missing data (stage, n = 2; response to therapy, n = 4; surgical debulking, n = 4; survival, n = 20).

[b] pT stage was not assessed for 4 cases.

[c] pN stage was not assessed for 49 cases; 47 of which were stage III/IV.

https://doi.org/10.1371/journal.pone.0256615.t002

median AQUA[®] scores of 308.9 and 152.6, respectively (p = 8.3x10^{-13}). However, within tumors, we observed the opposite of IHC analysis and found stromal Cav-1 expression was higher than in the epithelium with median AQUA[®] scores of 152.6 and 124.0, respectively (p = 0.01).

Cav-1 Desmoplastic Stroma AQUA® Score= 86.31

Cav-1 Normal Stroma AQUA® Score= 507.24
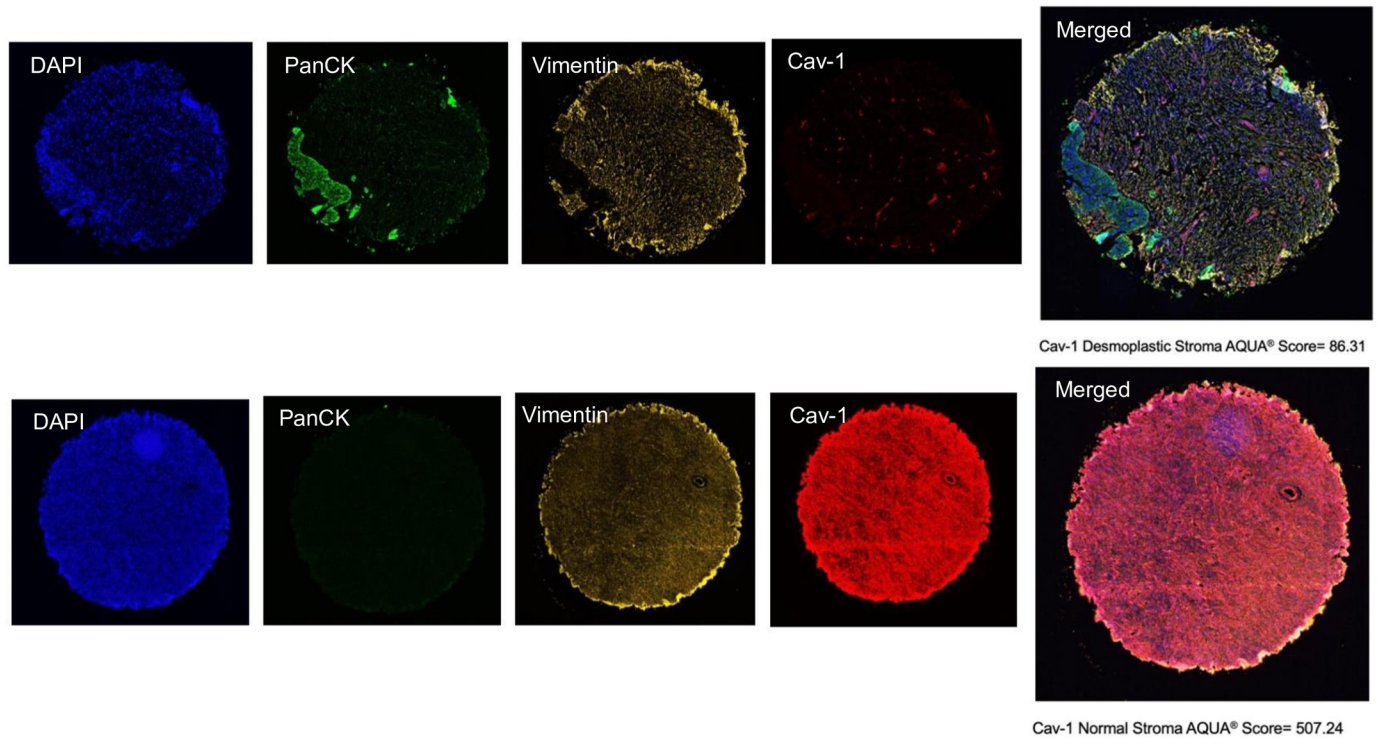
Fig 3. Multiplex immunofluorescent staining of ovarian tissues in Cohort 2. Representative staining for high-grade ovarian serous adenocarcinoma (top) and benign ovarian tissue (bottom) are provided. Compartmental regions were identified based on DAPI, PanCK, and DAPI staining. Tumor (desmoplastic) stroma regions comprised stromal cells (Vimentin+) with a nucleus (DAPI+), and not epithelial (panCK-).

https://doi.org/10.1371/journal.pone.0256615.g003

For 11 OvCa tissues quantified by both IF and IHC assays, we observed moderate correlation between methods for Cav-1 expression in stroma (pearson r^2 = 0.69, p = 0.006) whereas there was little correlation for the epithelium (pearson r^2 = 0.006, p = 0.98). Notably, 6 out 7 samples that had no stromal Cav-1 expression by IHC (Hscore = 0) had >100 AQUA scores (range = 102–200, S1A Fig). Among eight samples with moderate IHC expression of Cav-1 in the tumor epithelium (Hscore = 3), we observed a wide range of AQUA scores (range = 88–257, S1B Fig). Furthermore, stroma expression was only downregulated in 3 samples by IF assay but was downregulated in all samples by IHC (S1C Fig).

Stromal Cav-1 expression was significantly higher for cases over 65 years of age compared to those 65 years and younger (p = 0.03) while the expression in the epithelium did not differ by age (p = 0.23; Table 2). The high-grade tumors had lower expression of Cav-1 in both the stroma and epithelium compared to low-grade tumors; however, there were only 5 low-grade cases and the difference was not statistically significance (p = 0.55 and p = 0.14, respectively). Compared to optimally debulked tumors, suboptimal debulked tumors had a larger difference (downregulation) in epithelial Cav-1 (p = 0.04). Further, while Cav-1 expression did not vary by stage, stromal Cav-1 was significantly higher in tumors larger than 20mm (p = 0.04). Neither the stroma nor the epithelium expression differed by therapy response or survival groups.

For a subset of serous cases (n = 75), we pathologically reviewed and annotated tumor tissue for the presence of tumor infiltrating lymphocyte (TIL) aggregates, cystic component, and lymphovascular invasion (LVI) (see Methods). Analysis of Cav-1 expression by pathological characteristics (Table 3) detected a significantly higher epithelial expression of Cav-1 among serous tumors with TIL present compared to those without TIL (p = 0.04). In contrast, stromal Cav-1 expression did not differ by TIL presence (p = 0.94). Consequently, the difference

Table 3. Immunofluorescent Cav-1 expression in serous ovarian cancer by pathological characteristics in Cohort 2.

Pathological Characteristics	N (%)	Cav-1 Expression, median (SD)		Mean Δ (SD)
		Stroma	Epithelium	
Tumor infiltrating lymphocytes (TIL)				
No	43 (57%)	154.8 (39.1)	114.2 (39.6)	29.0 (34.4)
Yes	32 (43%)	153.0 (48.0)	138.7 (59.7)	6.4 (45.6)
		p = 0.94	**p = 0.04**	**p = 0.02**
Cystic Component				
No	23 (31%)	146.8 (41.5)	120.1 (37.2)	20.5 (29.1)
Yes	52 (69%)	155.2 (43.2)	124.2 (54.8)	18.8 (45.3)
		p = 0.23	p = 0.53	p = 0.85
Lymphovascular Invasion				
No	17 (23%)	146.8 (53.5)	122.5 (75.9)	1.4 (54.3)
Yes	58 (77%)	154.8 (39.3)	120.1 (38.6)	24.9 (34.6)
		p = 0.88	p = 0.63	p = 0.11

SD, standard deviation. P-values comparing Cav-1 expression by subgroups were calculated using Wilcoxon rank sum test. P-values for comparison of mean difference were calculated using Student's t-test.

https://doi.org/10.1371/journal.pone.0256615.t003

between stromal and epithelial expression of Cav-1 was significantly lower among tumors with TIL (p = 0.02). We did not detect differences in Cav-1 expression based on cystic component or lymphovascular invasion (Table 3).

For patients with low levels (< median) of epithelial Cav-1 expression, the median survival was 57.5 months compared to 50 months for those with high levels (≥ median) (log-rank p = 0.83, Fig 4A). For the stroma regions, the median survival was 62.2 months for patients with low levels of Cav-1 expression compared to 46.5 months for those with high levels (log-rank p = 0.16, Fig 4B). Cox-proportional hazards modeling of continuous Cav-1 expression with adjustment for age, stage, and response to therapy, found neither epithelial (HR = 1.00, 95% CI = 1.00–1.01, p = 0.81) or stromal (HR = 1.01, 95% CI = 1.00–1.01, p = 0.37) Cav-1
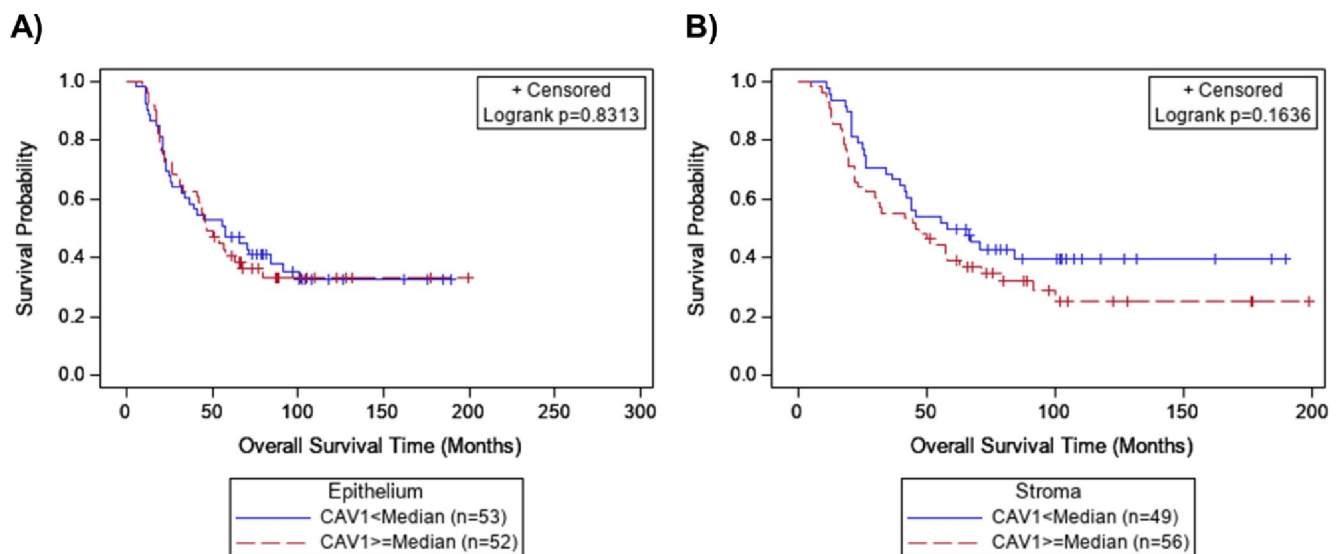
Fig 4. Overall survival of serous ovarian cancer by expression of Cav-1 in Cohort 2. Kaplan-Meier survival curves for Cohort 2 by immunofluorescent expression of Cav-1 in the (A) tumor epithelium and (B) stroma, using the median AQUA® score as the cutoff.

https://doi.org/10.1371/journal.pone.0256615.g004

expression were associated with patient survival (S2 Table). Among patients with pathological characteristic data, the presence of lymphovascular invasion was significantly associated with poorer survival (HR = 3.56, 95% CI = 1.51–8.38, p = 0.004) while TIL and cystic component were not (S3 Table). Cav-1 expression was not associated with survival in models adjusted for pathological characteristics (S3 Table).

Discussion

Ovarian cancer remains one of the most lethal gynecological malignancies, with most patients presenting with advanced stage tumors. Unfortunately, current standard treatment regimens are not optimal. Given the emerging importance of the tumor microenvironment with respect to carcinogenesis and chemoresistance, we evaluated the expression of Cav-1, a key potential regulator, specifically exploring its role in ovarian serous adenocarcinoma as a therapeutic and prognostic factor. Our results show that expression of Cav-1 is downregulated in OvCa stroma compared to benign stroma which was detected with both IHC and IF quantification methods. This finding is in-line with an intriguing paradigm of 'parasitic' tumor-stromal metabolism called the Reverse Warburg Effect (RWE) [33] which suggests that tumor cells 'hijack' CAFs by inducing oxidative stress and downregulating stromal Cav-1 to promote catabolic processes that supply nutrients to tumor cells for anabolic growth and survival thereby promoting tumor progression, metastasis, and resistance to therapy. We also found that Cav-1 is more highly expressed in the epithelium of serous tumors with TIL and that they have less Cav-1 stromal loss. CAFs have been shown to regulate T cells through secretion of IL-6 [34] suggesting the higher epithelial Cav-1 expression (and less stromal loss) reflects a tumor microenvironment with fewer CAFs and better immune response. Cav-1 and other markers of the RWE represent promising targets for new combinations of therapies that work by 'uncoupling' tumor cells from CAFs by preventing stromal Cav-1 degradation [35–39] which may also have the ability to attenuate immunosuppression for immune therapies. Our findings demonstrate that loss of Cav-1 expression in CAF-enriched stromal cells is a marker of malignant ovarian disease and suggest Cav-1 may be a therapeutic target for OvCa.

The expression of stromal Cav-1 relative to the epithelium varied by assay with IHC showing downregulation in stroma whereas IF showed upregulation. The difference may be due to tumor heterogeneity or an increased sensitivity and specificity of IF with digital image analysis. In the comparison of biological replicates, IF detected stromal Cav-1 expression in all 7 tissues that displayed no expression with IHC. We also observed a wide-range of epithelium Cav-1 expression detected with IF (88 to 258) for a single IHC Hscore (3). This could result from increased reliability of using objective image analysis versus potentially more subjective human observers. The human eye is more prone to errors when scoring stained slides due to the difference in each individual's perception of color and intensity and the context in which the human eye views an image, as well as fatigue; whereas, the machine uses individual pixel intensity to score a slide which is an intrinsic property of the image and is not influenced by its surrounding [32]. With the limited number of tissues quantified by both assays, we were unable to comprehensively compare methods. Further investigations are needed to better assess tumor heterogeneity, method concordance, and the limitations of TMA versus whole slide images. Given the advancements in digital pathology, future studies should be carried out to promote reproducibility; thus, allowing for improved precision of biomarker measurements in the field. In particular, the automated detection of regions of interest could improve the accuracy of detection and standardization [40].

With the IF assay, we were able to detect differences in Cav-1 expression across clinicopathologic characteristics. We observed higher expression of stromal Cav-1 with age in cohort 2.

Additionally, low-grade tumors appeared to have higher expression of Cav-1 than high-grade tumors, although we evaluated only 5 (5%) OvCa tissues given the rare prevalence of low-grade disease at diagnosis (5–10%) [41]. Based on the RWE, one could reasonably extrapolate that as a cancer becomes more aggressive there is more stromal metabolism, and as such, less Cav-1 in the surrounding stroma. However, we also observed a suggested trend (p = 0.08) of higher stromal Cav-1 expression among short-term survivors. Perhaps, in advanced stage tumors that are associated with shorter survival times, changing metabolic needs [42] and migration of aggressive tumor cells require less nutrients from the surrounding stroma, while in the early stage tumors which are associated with longer survival times, the tumor cells remain locally and deplete the surrounding stomal Cav-1. We also evaluated the association of Cav-1 expression with response to standard first-line platinum-based chemotherapy but did not detect a difference. Our study did not differentiate stroma based on desmoplastic reaction which may be an important determinant of Cav-1 expression and its association with clinical outcomes [43, 44]. The current findings, however, suggest a limited clinical utility for stromal Cav-1 expression as a biomarker for predicting chemotherapy response. Overall, the Cav-1 expression levels in the tumor microenvironment are quantifiable via digital image analysis and could potentially serve as a diagnostic biomarker assay. Given that only malignant (or benign) cases were assessed, future studies should be undertaken to explore the utility of Cav-1 in more diagnostically challenging, "borderline" ovarian neoplasms. In-line with previous studies [12–14, 26], the statistically significantly higher expression of Cav-1 in the benign stroma versus tumor stroma demonstrates that Cav-1 may play an important role in carcinogenesis and further studies may provide insight into the evolutionary biology of OvCa. Although the utility in predicting response to standard platinum-based chemotherapy was limited, Cav-1 could prove to be an interesting therapeutic target based on its loss in malignant ovarian tissue. Studies are needed to glean mechanistic insights into how reduced levels of Cav-1 in the stroma may promote transformation to ovarian carcinoma.

Our findings demonstrate that loss of desmoplastic stromal Cav-1expression may be associated with malignant ovarian serous carcinomas. Studies are needed to replicate these findings and explore mechanisms that can be targeted to reduce progression to malignancy.

Supporting information

S1 File. Supplementary IF staining methods.
(DOCX)

S2 File. Clinicopathologic and Cav-1 expression data for Cohort 1 and Cohort 2.
(XLS)

S1 Fig. Comparison of Cav-1 expression quantified by immunofluorescence and immunohistochemistry.
(DOCX)

S1 Table. Association of Cav-1 expression with overall survival of serous ovarian cancer in Cohort 1.
(DOCX)

S2 Table. Association of Cav-1 expression with overall survival of serous ovarian cancer in Cohort 2.
(DOCX)

S3 Table. Association of pathological features with overall survival of serous ovarian cancer.
(DOCX)

Acknowledgments

The authors wish to thank the study participants for donating tissue and data for this project.

Author Contributions

Conceptualization: Anthony M. Magliocco, Jennifer B. Permuth.

Data curation: Daryoush Saeed-Vafa, Douglas C. Marchion, Susan M. McCarthy, Ardeshir Hakam, Alexis Lopez, Dung-Tsa Chen, Brett M. Reid, Jennifer B. Permuth.

Formal analysis: Daryoush Saeed-Vafa, Douglas C. Marchion, Susan M. McCarthy, Ardeshir Hakam, Alexis Lopez, Dung-Tsa Chen, Brett M. Reid, Jennifer B. Permuth.

Funding acquisition: Johnathan M. Lancaster, Jennifer B. Permuth.

Investigation: Daryoush Saeed-Vafa, Douglas C. Marchion, Susan M. McCarthy, Ardeshir Hakam, Alexis Lopez, Robert M. Wenham, Sachin M. Apte, Dung-Tsa Chen, Anthony M. Magliocco, Brett M. Reid, Jennifer B. Permuth.

Methodology: Daryoush Saeed-Vafa, Anthony M. Magliocco, Brett M. Reid, Jennifer B. Permuth.

Project administration: Daryoush Saeed-Vafa, Brett M. Reid, Jennifer B. Permuth.

Resources: Johnathan M. Lancaster, Jennifer B. Permuth.

Software: Daryoush Saeed-Vafa.

Supervision: Anthony M. Magliocco, Johnathan M. Lancaster, Jennifer B. Permuth.

Validation: Daryoush Saeed-Vafa, Douglas C. Marchion, Susan M. McCarthy, Ardeshir Hakam, Alexis Lopez, Dung-Tsa Chen, Brett M. Reid, Jennifer B. Permuth.

Visualization: Daryoush Saeed-Vafa.

Writing – original draft: Daryoush Saeed-Vafa, Anthony M. Magliocco, Brett M. Reid, Jennifer B. Permuth.

Writing – review & editing: Daryoush Saeed-Vafa, Douglas C. Marchion, Susan M. McCarthy, Ardeshir Hakam, Alexis Lopez, Robert M. Wenham, Sachin M. Apte, Dung-Tsa Chen, Anthony M. Magliocco, Brett M. Reid, Jennifer B. Permuth.

References

1. American Cancer Society. Cancer Facts & Figures 2018 2018 [cited 2018]. Available from: https://www.cancer.org/content/dam/cancer-org/research/cancer-facts-and-statistics/annual-cancer-facts-and-figures/2018/cancer-facts-and-figures-2018.pdf.

2. Schauer IG, Sood AK, Mok S, Liu J. Cancer-associated fibroblasts and their putative role in potentiating the initiation and development of epithelial ovarian cancer. Neoplasia (New York, NY). 2011; 13 (5):393–405. Epub 2011/05/03. https://doi.org/10.1593/neo.101720 PMID: 21532880; PubMed Central PMCID: PMC3084616.

3. Labiche A, Heutte N, Herlin P, Chasle J, Gauduchon P, Elie N. Stromal compartment as a survival prognostic factor in advanced ovarian carcinoma. International journal of gynecological cancer: official journal of the International Gynecological Cancer Society. 2010; 20(1):28–33. Epub 2010/02/05. https://doi.org/10.1111/IGC.0b013e3181bda1cb PMID: 20130500.

4. Kataoka F, Tsuda H, Arao T, Nishimura S, Tanaka H, Nomura H, et al. EGRI and FOSB gene expressions in cancer stroma are independent prognostic indicators for epithelial ovarian cancer receiving standard therapy. Genes, chromosomes & cancer. 2012; 51(3):300–12. Epub 2011/11/19. https://doi.org/10.1002/gcc.21916 PMID: 22095904.

5. Lai D, Ma L, Wang F. Fibroblast activation protein regulates tumor-associated fibroblasts and epithelial ovarian cancer cells. International journal of oncology. 2012; 41(2):541–50. Epub 2012/05/23. https://doi.org/10.3892/ijo.2012.1475 PMID: 22614695.

6. Zhang Y, Tang H, Cai J, Zhang T, Guo J, Feng D, et al. Ovarian cancer-associated fibroblasts contribute to epithelial ovarian carcinoma metastasis by promoting angiogenesis, lymphangiogenesis and tumor cell invasion. Cancer letters. 2011; 303(1):47–55. Epub 2011/02/12. https://doi.org/10.1016/j.canlet.2011.01.011 PMID: 21310528.

7. Steg AD, Katre AA, Goodman B, Han HD, Nick AM, Stone RL, et al. Targeting the notch ligand JAGGED1 in both tumor cells and stroma in ovarian cancer. Clinical cancer research: an official journal of the American Association for Cancer Research. 2011; 17(17):5674–85. Epub 2011/07/15. https://doi.org/10.1158/1078-0432.CCR-11-0432 PMID: 21753153; PubMed Central PMCID: PMC3166981.

8. Davidson B, Goldberg I, Givant-Horwitz V, Nesland JM, Berner A, Bryne M, et al. Caveolin-1 expression in ovarian carcinoma is MDR1 independent. American journal of clinical pathology. 2002; 117(2):225–34. Epub 2002/02/28. https://doi.org/10.1309/u40r-1bn4-6kj3-bdg3 PMID: 11863219.

9. Davidson B, Nesland JM, Goldberg I, Kopolovic J, Gotlieb WH, Bryne M, et al. Caveolin-1 expression in advanced-stage ovarian carcinoma—a clinicopathologic study. Gynecologic oncology. 2001; 81 (2):166–71. Epub 2001/05/02. https://doi.org/10.1006/gyno.2001.6156 PMID: 11330944.

10. Quann K, Gonzales DM, Mercier I, Wang C, Sotgia F, Pestell RG, et al. Caveolin-1 is a negative regulator of tumor growth in glioblastoma and modulates chemosensitivity to temozolomide. Cell cycle (Georgetown, Tex). 2013; 12(10):1510–20. Epub 2013/04/20. https://doi.org/10.4161/cc.24497 PMID: 23598719; PubMed Central PMCID: PMC3680531.

11. Wiechen K, Diatchenko L, Agoulnik A, Scharff KM, Schober H, Arlt K, et al. Caveolin-1 is down-regulated in human ovarian carcinoma and acts as a candidate tumor suppressor gene. The American journal of pathology. 2001; 159(5):1635–43. Epub 2001/11/07. https://doi.org/10.1016/S0002-9440(10)63010-6 PMID: 11696424; PubMed Central PMCID: PMC1867061.

12. Witkiewicz AK, Dasgupta A, Sotgia F, Mercier I, Pestell RG, Sabel M, et al. An absence of stromal caveolin-1 expression predicts early tumor recurrence and poor clinical outcome in human breast cancers. The American journal of pathology. 2009; 174(6):2023–34. Epub 2009/05/05. https://doi.org/10.2353/ajpath.2009.080873 PMID: 19411448; PubMed Central PMCID: PMC2684168.

13. Di Vizio D, Morello M, Sotgia F, Pestell RG, Freeman MR, Lisanti MP. An absence of stromal caveolin-1 is associated with advanced prostate cancer, metastatic disease and epithelial Akt activation. Cell cycle (Georgetown, Tex). 2009; 8(15):2420–4. Epub 2009/06/27. https://doi.org/10.4161/cc.8.15.9116 PMID: 19556867; PubMed Central PMCID: PMC2927821.

14. Shan T, Lu H, Ji H, Li Y, Guo J, Chen X, et al. Loss of stromal caveolin-1 expression: a novel tumor microenvironment biomarker that can predict poor clinical outcomes for pancreatic cancer. PloS one. 2014; 9(6):e97239. Epub 2014/06/21. https://doi.org/10.1371/journal.pone.0097239 PMID: 24949874; PubMed Central PMCID: PMC4064978.

15. Campbell L, Gumbleton M, Griffiths DF. Caveolin-1 overexpression predicts poor disease-free survival of patients with clinically confined renal cell carcinoma. British journal of cancer. 2003; 89(10):1909–13. Epub 2003/11/13. https://doi.org/10.1038/sj.bjc.6601359 PMID: 14612902; PubMed Central PMCID: PMC2394459.

16. Ayala G, Morello M, Frolov A, You SY, Li RL, Rosati F, et al. Loss of caveolin-1 in prostate cancer stroma correlates with reduced relapse-free survival and is functionally relevant to tumour progression. J Pathol. 2013; 231(1):77–87. https://doi.org/10.1002/path.4217 WOS:000322761500009. PMID: 23729330

17. Bonuccelli G, Whitaker-Menezes D, Castello-Cros R, Pavlides S, Pestell RG, Fatatis A, et al. The reverse Warburg effect: glycolysis inhibitors prevent the tumor promoting effects of caveolin-1 deficient cancer associated fibroblasts. Cell cycle (Georgetown, Tex). 2010; 9(10):1960–71. Epub 2010/05/25. https://doi.org/10.4161/cc.9.10.11601 PMID: 20495363.

18. Rossi S, Poliani PL, Cominelli M, Bozzato A, Vescovi R, Monti E, et al. Caveolin 1 is a marker of poor differentiation in Rhabdomyosarcoma. European journal of cancer (Oxford, England: 1990). 2011; 47 (5):761–72. Epub 2010/11/26. https://doi.org/10.1016/j.ejca.2010.10.018 PMID: 21106364.

19. Simpkins SA, Hanby AM, Holliday DL, Speirs V. Clinical and functional significance of loss of caveolin-1 expression in breast cancer-associated fibroblasts. The Journal of pathology. 2012; 227(4):490–8. Epub 2012/04/11. https://doi.org/10.1002/path.4034 PMID: 22488553.

20. Paskas S, Jankovic J, Marecko I, Isic Dencic T, Tatic S, Cvejic D, et al. Caveolin-1 expression in papillary thyroid carcinoma: correlation with clinicopathological parameters and BRAF mutation status. Otolaryngology—head and neck surgery: official journal of American Academy of Otolaryngology-Head and Neck Surgery. 2014; 150(2):201–9. Epub 2013/11/21. https://doi.org/10.1177/0194599813512781 PMID: 24255086.

21. Hu J, Shao SJ, Song Y, Zhao JY, Dong Y, Gong LL, et al. Hepatocyte Growth Factor Induces Invasion and Migration of Ovarian Cancer Cells by Decreasing the Expression of E-Cadherin, beta-Catenin, and Caveolin-1. Anat Rec. 2010; 293(7):1134–9. https://doi.org/10.1002/ar.21147 WOS:000280316800004. PMID: 20583256

22. Prinetti A, Cao T, Illuzzi G, Prioni S, Aureli M, Gagliano N, et al. A Glycosphingolipid/Caveolin-1 Signaling Complex Inhibits Motility of Human Ovarian Carcinoma Cells. J Biol Chem. 2011; 286(47):40900–10. https://doi.org/10.1074/jbc.M111.286146 WOS:000297315400050. PMID: 21949119

23. Syed V, Mukherjee K, Lyons-Weiler J, Lau KM, Mashima T, Tsuruo T, et al. Identification of ATF-3, caveolin-1, DLC-1, and NM23-H2 as putative antitumorigenic, progesterone-regulated genes for ovarian cancer cells by gene profiling. Oncogene. 2005; 24(10):1774–87. https://doi.org/10.1038/sj.onc.1207991 WOS:000227345100013. PMID: 15674352

24. Bagnoli M, Tomassetti A, Figini M, Flati S, Dolo V, Canevari S, et al. Downmodulation of caveolin-1 expression in human ovarian carcinoma is directly related to alpha-folate receptor overexpression. Oncogene. 2000; 19(41):4754–63. Epub 2000/10/14. https://doi.org/10.1038/sj.onc.1203839 PMID: 11032026.

25. Kai WC, Diatchenko L, Agoulnik A, Scharff KM, Schober H, Arlt K, et al. Caveolin-1 is down-regulated in human ovarian carcinoma and acts as a candidate tumor suppressor gene. American Journal of Pathology. 2001; 159(5):1635–43. https://doi.org/10.1016/S0002-9440(10)63010-6 WOS:000171988000006.

26. Sayhan S, Diniz G, Karadeniz T, Ayaz D, Kahraman DS, Gokcu M, et al. Expression of caveolin-1 in peritumoral stroma is associated with histological grade in ovarian serous tumors. Ginekologia polska. 2015; 86(6):424–8. Epub 2015/08/11. https://doi.org/10.17772/gp/2398 PMID: 26255449.

27. Ghaznavi F, Evans A, Madabhushi A, Feldman M. Digital imaging in pathology: whole-slide imaging and beyond. Annual review of pathology. 2013; 8:331–59. Epub 2012/11/20. https://doi.org/10.1146/annurev-pathol-011811-120902 PMID: 23157334.

28. Permuth-Wey J, Sellers TA. Epidemiology of ovarian cancer. Methods in molecular biology (Clifton, NJ). 2009; 472:413–37. Epub 2008/12/25. https://doi.org/10.1007/978-1-60327-492-0_20 PMID: 19107446.

29. Rizzardi AE, Johnson AT, Vogel RI, Pambuccian SE, Henriksen J, Skubitz AP, et al. Quantitative comparison of immunohistochemical staining measured by digital image analysis versus pathologist visual scoring. Diagnostic pathology. 2012; 7:42. Epub 2012/04/21. https://doi.org/10.1186/1746-1596-7-42 PMID: 22515559; PubMed Central PMCID: PMC3379953.

30. Pietras K, Ostman A. Hallmarks of cancer: interactions with the tumor stroma. Experimental cell research. 2010; 316(8):1324–31. Epub 2010/03/10. https://doi.org/10.1016/j.yexcr.2010.02.045 PMID: 20211171.

31. Allen M, Louise Jones J. Jekyll and Hyde: the role of the microenvironment on the progression of cancer. The Journal of pathology. 2011; 223(2):162–76. Epub 2010/12/03. https://doi.org/10.1002/path.2803 PMID: 21125673.

32. Gustavson M, Dolled-Filhart M, Christiansen J, Pinard R, Rimm D. Aqua technology and molecular pathology. In: Platero JS, editor. Molecular Pathology in Drug Discovery and Development. Hoboken, NJ: John Wiley & Sons; 2009. p. 295–334.

33. Martinez-Outschoorn UE, Balliet RM, Rivadeneira DB, Chiavarina B, Pavlides S, Wang C, et al. Oxidative stress in cancer associated fibroblasts drives tumor-stroma co-evolution: A new paradigm for understanding tumor metabolism, the field effect and genomic instability in cancer cells. Cell cycle (Georgetown, Tex). 2010; 9(16):3256–76. Epub 2010/09/04. https://doi.org/10.4161/cc.9.16.12553 PMID: 20814239; PubMed Central PMCID: PMC3041164.

34. Kato T, Noma K, Ohara T, Kashima H, Katsura Y, Sato H, et al. Cancer-Associated Fibroblasts Affect Intratumoral CD8(+) and FoxP3(+) T Cells Via IL6 in the Tumor Microenvironment. Clinical cancer research: an official journal of the American Association for Cancer Research. 2018; 24(19):4820–33. Epub 2018/06/21. https://doi.org/10.1158/1078-0432.CCR-18-0205 PMID: 29921731.

35. Chan DK, Miskimins WK. Metformin and phenethyl isothiocyanate combined treatment in vitro is cytotoxic to ovarian cancer cultures. Journal of ovarian research. 2012; 5(1):19. Epub 2012/07/12. https://doi.org/10.1186/1757-2215-5-19 PMID: 22781119; PubMed Central PMCID: PMC3439343.

36. Rattan R, Graham RP, Maguire JL, Giri S, Shridhar V. Metformin suppresses ovarian cancer growth and metastasis with enhancement of cisplatin cytotoxicity in vivo. Neoplasia (New York, NY). 2011; 13

(5):483–91. Epub 2011/05/03. https://doi.org/10.1593/neo.11148 PMID: 21532889; PubMed Central PMCID: PMC3084625.

37. Secord AA, Teoh DK, Barry WT, Yu M, Broadwater G, Havrilesky LJ, et al. A phase I trial of dasatinib, an SRC-family kinase inhibitor, in combination with paclitaxel and carboplatin in patients with advanced or recurrent ovarian cancer. Clinical cancer research: an official journal of the American Association for Cancer Research. 2012; 18(19):5489–98. Epub 2012/07/28. https://doi.org/10.1158/1078-0432.ccr-12-0507 PMID: 22837181; PubMed Central PMCID: PMC3463759.

38. Teoh D, Ayeni TA, Rubatt JM, Adams DJ, Grace L, Starr MD, et al. Dasatinib (BMS-35482) has synergistic activity with paclitaxel and carboplatin in ovarian cancer cells. Gynecologic oncology. 2011; 121 (1):187–92. Epub 2011/01/07. https://doi.org/10.1016/j.ygyno.2010.11.017 PMID: 21208651; PubMed Central PMCID: PMC3062679.

39. Loar P, Wahl H, Kshirsagar M, Gossner G, Griffith K, Liu JR. Inhibition of glycolysis enhances cisplatin-induced apoptosis in ovarian cancer cells. American journal of obstetrics and gynecology. 2010; 202 (4):371.e1-8. Epub 2010/02/09. https://doi.org/10.1016/j.ajog.2009.10.883 PMID: 20138251.

40. Patil SM, Tong L, Wang MD. Generating Region of Interests for Invasive Breast Cancer in Histopathological Whole-Slide-Image. Proc COMPSAC. 2020; 2020:723–8. Epub 2020/10/09. https://doi.org/10.1109/compsac48688.2020.0-174 PMID: 33029594; PubMed Central PMCID: PMC7537355.

41. Martinez-Outschoorn UE, Balliet RM, Lin Z, Whitaker-Menezes D, Howell A, Sotgia F, et al. Hereditary ovarian cancer and two-compartment tumor metabolism: epithelial loss of BRCA1 induces hydrogen peroxide production, driving oxidative stress and NFkappaB activation in the tumor stroma. Cell cycle (Georgetown, Tex). 2012; 11(22):4152–66. Epub 2012/10/11. https://doi.org/10.4161/cc.22226 PMID: 23047606; PubMed Central PMCID: PMC3524211.

42. Weber GF. Time and Circumstances: Cancer Cell Metabolism at various Stages of Disease Progression. Front Oncol. 2016; 6. ARTN 257 https://doi.org/10.3389/fonc.2016.00257 WOS:000389661500001.

43. Ueno H, Kajiwara Y, Ajioka Y, Sugai T, Sekine S, Ishiguro M, et al. Histopathological atlas of desmoplastic reaction characterization in colorectal cancer. Jpn J Clin Oncol. 2021; 51(6):1004–12. Epub 2021/04/16. https://doi.org/10.1093/jjco/hyab040 PMID: 33855369; PubMed Central PMCID: PMC8193706.

44. Wernicke M, Pineiro LC, Caramutti D, Dorn VG, Raffo MM, Guixa HG, et al. Breast cancer stromal myxoid changes are associated with tumor invasion and metastasis: a central role for hyaluronan. Mod Pathol. 2003; 16(2):99–107. Epub 2003/02/20. https://doi.org/10.1097/01.MP.0000051582.75890.2D PMID: 12591961.